New evidence for the incision history of the Liuchong River, Southwest China, from cosmogenic ^{26}Al/^{10}Be burial ages in cave sediments

Yu Liu [a,b], Shijie Wang [a,c,*], Sheng Xu [d], Xiuming Liu [a,c], Derek Fabel [e], Xinbao Zhang [f], Weijun Luo [a,c], Anyun Cheng [a,c]

[a] State Key Laboratory of Environmental Geochemistry, Institute of Geochemistry, Chinese Academy of Sciences, Guiyang 550002, China
[b] University of Chinese Academy of Sciences, Beijing 100049, China
[c] Puding Karst Ecosystem Research Station, CAS, Puding 562100, China
[d] Scottish Universities Environmental Research Centre, East Kilbride G750 QF, UK
[e] Department of Earth Science and Geography, University of Glasgow, Glasgow G12 8QQ, UK
[f] Institute of Mountain Hazards and Environment, CAS, Chengdu 610041, China

ABSTRACT

Cosmogenic nuclides ^{10}Be and ^{26}Al have been analyzed for sediments from the multilevel riverside caves along the Liuchong River at the southeastern margin of the Tibetan Plateau. The Liuchong River is the northern origin of Wujiang River, which passes through the northwestern Guizhou Plateau and cuts down hundreds of meters into the bedrock, leaving behind an abundance of multilevel caves. The measured ^{26}Al/^{10}Be ratios produced the apparent burial ages in range of 0.49–2.85 Ma. Taking into account of geomorphic and geological backgrounds, the Dashi Cave located at the highest level along the Liuchong River system formed around 0.75 Ma ago, which probably suggests the initial formation age of the modern Wujiang River. The resulted incision rate of ~480 m/Ma in Guizhou in the last 0.75 Ma is slightly higher than those in adjacent areas. This feature implies an intensive downcutting history of the Liuchong River during the Quaternary, which might be primarily caused by the uplift of Tibetan Plateau, cut-through of the Three Gorges and soluble carbonate bedrock.

© 2013 Elsevier Ltd. All rights reserved.

1. Introduction

Guizhou Plateau is located on the southeastern edge of the Tibetan Plateau, which is an important geomorphic transition zone of China (Fig. 1A). For half a century, the landscape evolution of Guizhou during the late Cenozoic has been a much debated topic in the Earth sciences due to poorly preserved surface materials and unsuitable dating methods. It is unclear how the timing and amount of uplift of Guizhou Plateau during the late Cenozoic era. Many studies regarded the uplift of the Guizhou as profoundly influenced by the rapid uplift of the Tibetan Plateau during the late Pliocene or early Quaternary (GGMB, 1987; Zhou and Chen, 1993; Lin et al., 1994; Li, 2001). However, the quantitative analysis of Guizhou Plateau uplift history remains very scarce. Only a few studies have investigated the uplift history and landscape evolution of Guizhou by employing the speleothem U-series method (Zhang and Zhao, 1985; Yang, 1998; Li et al., 2007). Because of

the limitation of U-series geochronology, the oldest speleothem age is only known to be more than 350 ka (Yang, 1998).

The Guizhou landscape is characterized by stepped landforms (planation surfaces, fluvial terraces and caves) that are well developed. The age and elevation of the stepped landforms are recognized as an important field for the studies of land uplift history and landscape evolution. Dating the age of planation surfaces is very difficult in Guizhou because of the lack of volcanic ash or other suitable dating materials. However, measuring river down-cutting rate from terraces is particularly problematic in karst terrain because terraces may be degraded by carbonate dissolution and sinkhole collapse (Granger et al., 1997). Moreover, most terraces of the primary rivers in Guizhou are erosional terraces, which rarely have suitable materials for dating. Nevertheless, riverside caves can record river levels, either as repositories of river sediments or through calcite formations that form only above the water table. Fine sediment paleomagnetism and speleothem U-series method are the common dating methods of cave ages, besides the limitation of age range, these two dating methods may lead to the misidentification of cave ages (Partriage et al., 2003; Stock et al., 2005a).

Today, a new method of absolute age dating, called cosmogenic nuclide dating, offers an opportunity to solve these problems. First,

---

* Corresponding author at: State Key Laboratory of Environmental Geochemistry, Institute of Geochemistry, Chinese Academy of Sciences, Guiyang 550002, China. Tel.: +86 851 5891338; fax: +86 851 5891609.

E-mail address: wangshijie@vip.skleg.cn (S. Wang).

this method has a more extensive age range, from c. 0.1 to 5.5 Ma (Granger et al., 1997; Anthony and Granger, 2004). It is considered to be the most reliable method for dating cave developments in mountainous regions (Stock et al., 2005a). Cosmogenic burial age dating employs the measurement of two isotopes (generally ^{10}Be and ^{26}Al) in a sample that was initially exposed and then shielded from cosmic rays to determine the burial age of the sample. During the last decade, the use of this method has increased. For example, Granger et al. (1997, 2001), Stock et al. (2005b), Anthony and Granger (2004, 2007), Haeuselmann et al. (2007) and Wagner et al. (2010) analyzed ^{10}Be and ^{26}Al in alluvial sediments trapped in caves to interpret the Plio-Pleistocene history of river incision and tectonic uplift in various part of the world. Wolkowinsky and Granger (2004), Matmon et al. (2005, 2012), Kong et al. (2009), Hu et al. (2011) and Enlanger et al. (2012) used a similar approach in fluvial sediments and terraces that dated between 0.2 and 4.8 Ma. Moreover, cosmogenic nuclide burial dating also used in buried paleosols to date glacial sediments for understanding the development of the glacier (Balco et al., 2005; Balco and Rovey, 2008).

In this work, we dated caves in canyon walls using ^{26}Al/^{10}Be burial dating of quartzose sediments from the Liuchong River, the northern origin of Wujiang River, as the first evidence for a young incision history of the major drainage system of Guizhou Plateau. Combined with previous studies of speleothem U-series ages, we aim to discuss the incision history and landscape evolution of the study area.

2. Geological setting

The Guizhou Plateau is a east-tilted plateau with a mean altitude of ~1100 m, and the highest mountain in the west has an altitude of 2900 m. A series of stepped landforms exist in this area. These landforms are characterized by multilevel planation surfaces, fluvial terraces and caves that record the episodic uplift of Guizhou Plateau. Yang (1944) first proposed that there were three stages of Guizhou landscape evolution according to observations of concordant elevations of mountains. The study noted that each stage of evolution had a typical deplanation surface, including the Daloushan, Shanpen and Wujiang stages, which belong to the Paleogene, Neogene and Quaternary, respectively.

The Wujiang Stage denotes the incision of Wujiang River (25°56′–30°22′N, 104°10′–109°12′E), which is the largest river in Guizhou and the largest tributary of the Yangtze River from the south. During this stage, the entrenchment and aggradation of the river usually developed 4–5 level fluvial terraces and caves in the valley of primary rivers and carbonate rock area, respectively. The Wujiang River originates on Wumeng Mountain, flowing across the northern part of Guizhou Plateau and merging into the Yangtze River at Chongqing (Fig. 1A). The sedimentation of the
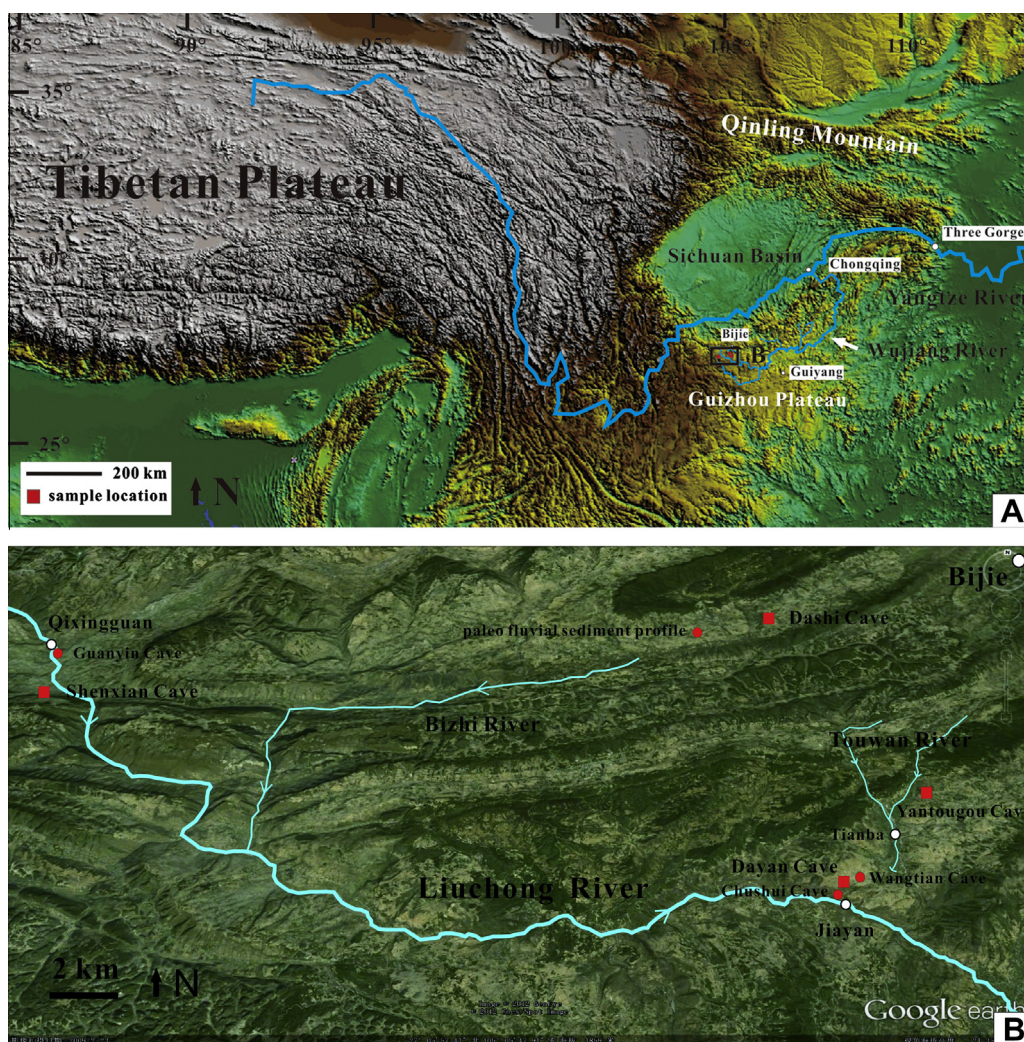

Fig. 1. Locality and distribution of the sampled caves. (A) Location of the Wujiang River in China; (B) sample location at the Liuchong River study area.

whole Wujiang River drainage basin is well developed, and the emergence of the stratum is quite complete. Carbonate rocks are about 60% of land area (GGMB, 1987), resulting in a well developed karst landform in Guizhou.

The Liuchong River, the northern origin of Wujiang River, flows across the northwestern part of the Guizhou Plateau and deeply cuts 300–400 m into the surface rock, leaving about six level caves in the river canyon wall at the Bijie area. The summit surface is a residual Tertiary planation surface with gentle hills and inter-mountain evolutional depressions with altitudes ranging from 1700 to 1800 m with a few up to 2000 m. In general, there are six multilevel caves (levels A–F) along the Liuchong River. The caves located at 320–350 m above the modern river level (AML) (level A) developed during a period when the Liuchong River flowed at the elevation of the northwestern part of the Guizhou Plateau. These caves mark the highest cave passage in this area, and they might correspond to the fourth terrace (erosional terrace) of Liuchong River. The cave passages at 220–250 m AML are the second level (level B) of this area. The cave passages at 120–140 m AML (level C) correspond to the third terrace (erosional terrace), and the cave passages at 50–70 m AML (level D) are the fourth level. The cave passages at 25–30 m AML (level E) are the fifth level and correspond to the second terrace (rock-seated terrace) of Liuchong River. These cave levels are hydrologically abandoned and are above the modern flood zone. The cave passages at 5–10 m AML (level F) are hydrologically active, correspond to smaller, discontinuous terraces above the modern floodplain and are still within the modern flood zone.

3. Site descriptions

This study covered the ~30 km river section between Jiayan and Qixingguan (Fig. 1B), along which five multilevel caves have developed (Fig. 2). The river surface altitude of this area is approximately 1200 m. At Jiayan, there are three level caves developed on the Liuchong River canyon wall. Wangtian Cave (WTC, level B) is the highest (1432 m a.s.l.) main riverside cave of this section. It is a relatively large cave with >10 m high, 6–7 m wide, and ~100 m long. The visible passage is nearly flat and straight. Although it is so hard to explore due to the serious collapse, we can evaluate this cave probably the drainage outlet to the main-stem of the upland. Dayan Cave (DYC, level C) is located ~90 m beneath the WTC, the cave entrance is face to the downstream direction of Liuchong River and the passage is developed toward the upstream. As described in Table 1, DYC is considered to be likely formed by the river lateral erosion in the backwater area due to the cave morphology and topographic feature. Besides, nearly 100 m below the DYC, Chushui Cave developed at level E.

It is also a large cave with 20 m high, 30 m wide and 30 m long, and ~30 m above the modern river. There are well rounded limestone and sandstone pebbles (mostly >10 cm) in the cave, but we did not collect the protogenic sample because the serious collapse and intensive human activity. At Qixingguan, Shenxian Cave (SXC) with 1420 m a.s.l. could be regarded as the same level of WTC (Fig. 2). Then, Guanyin Cave (level F) is under the Qixingguan Bridge and above the water surface ~5 m.

Dashi Cave (DSC) and Yantougou Cave (YTGC) are away from main stem of Liuchong River canyon, and belong to the Bizhi River and Touwan River area respectively, both of which are the tributaries of Liuchong River (Fig. 1B). The flow direction of Bizhi River is opposite to the main stem and turn almost right angle flow into the Liuchong River (Fig. 1B). Touwan River flows across the Tianba polje and dives into the ground at the edge of polje and become a underground river (Fig. 1B). DSC with the altitude of 1562 m is located at the highest level (level A) near the main stem canyon. It is at the bottom of the valley and the detailed description of DSC is in Table 1. YTGC is located in the Tianba polje, next to the main stem valley. Although it is lower than DSC, we attribute this cave to level A. Like DYC, entrance of YTGC is face to the downstream direction of Touwan River, we consider this cave as the lateral erosion by the tributary due to the cave morphology and topographic feature.

4. Material and methods

4.1. Sample collection and preparation

A total of more than 80 caves were investigated along the Wujiang River drainage basin. In previous work, only four caves and five coarse sediment samples (quartz pebbles and sand) collected from the Liuchong River were suitable for cosmogenic nuclide burial dating (Fig. 1B). The samples were deeply buried in caves (>20 m), besides the sample of Dayan Cave was collected from a deposit of branch cave that parallel to the main cave, the others were found in main open-channel deposits. The description of sampling site is in Table 1. These identified caves are morphologies clearly linking them to former river positions and they were positioned well downstream of glacial limits, where canyon cutting has been accomplished solely by river incision processes. Additionally, three cobble samples were collected from the modern river bank outside the caves to test for the presence of inherited burial signals in the samples collected in the caves.

Approximately 500 g of sandstone pebbles or sand were collected at each sampling site. Rock crushing and sieving were performed at the State Key Laboratory of Environmental Geochemistry, Institute of Geochemistry, Chinese Academy of Sciences. Quartz purification, Be and Al extraction and measurement
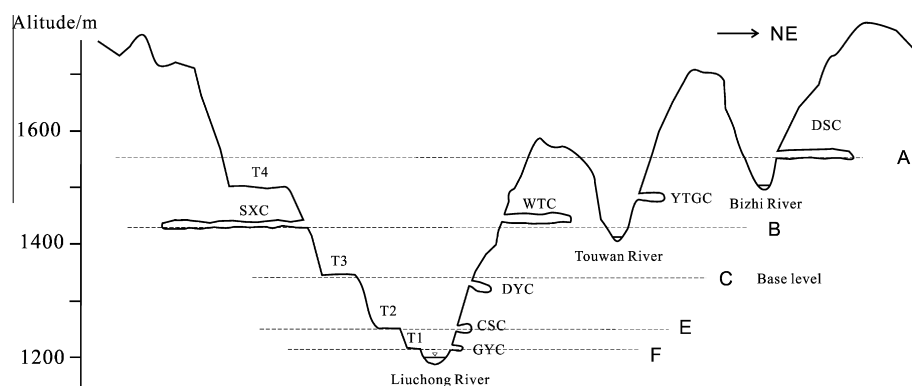

Fig. 2. Projected schematic view of cave system of study area. Inferred palaeowater table shown as dashed lines.

Table 1
Sample locations and descriptions of the study cave morphology and sampling section.

	Latitude (N)	Longitude (E)	Elevation (m a.s.l.)	Height above Liuchong River (m)	Cave morphology					Sampling section and sample description	
					Length (m)	Width (m)	Height (m)	Description	Type		
DSC	27°11′59.8″	105°12′07.3″	1562	362 ± 5	100	10	5	The cave is at the bottom of valley. Conduit trend is east by north, cave passage is flat and there was a slight collapse phenomenon	Water table cave	The thickness of section is ~30 cm, with obvious fluvial dual structure. The thickness of lower cobbles is ~20 cm, and the upper sand is ~10 cm. The lithology of pebbles contain limestone, purple mudstone and off white sandstone	The diameter of sandstone pebbles is ~1–3 cm, and pebbles are well rounded
YTGC	27°06′35.3″	105°12′34.2″	1488	288 ± 5	20	5	5	The passage is flat and near north to south, and gradually tighten to a small branch but cannot see the bottom, no collapse phenomenon	Lateral erosion cave	The sampling site is on the both sides wall which ~1–2 m from the cave ground and on the roof of the cave. The lithology of pebbles are primarily limestone, fine sandstone and sandstone, etc.	The diameter of sandstone pebbles is ~0.5–4 cm, and pebbles are rounded
DYC	27°04′24.8″	105°11′04.5″	1345	145 ± 5	50	5	5	The passage is near east to west, and about 15° downward sloping. There developed a branch cave (20 m length, 1 m width and 1 m height) beside the north of main conduit, and parallel to the main conduit	Lateral erosion cave	The sampling section is at the bottom of the branch cave. The thickness of section is ~30 cm, and the breakdown is cover on the top of section. The lithology of pebbles are primarily sandstone and cemented with sand	The diameter of sandstone pebbles is ~0.5–3 cm, and pebbles are well rounded
SXC	27°08′04.2″	104°57′10.3″	1420	220 ± 5	300	10	10	The passage is flat and straight and near east to west. The speleothem is well developed, and collapse phenomenon is few	Water table cave	The thickness of section is ~5 m, the diameter of pebbles are between 1 and 20 cm, cobbles are subangular to subrounded and mixed together with poorly sorted	The diameter of sandstone pebbles is ~3–5 cm, and pebbles are rounded
DSC bank	27°12′40.7″	105°13′13.2″	1512	312 ± 5						The pebbles are mostly 5–10 cm in size. The lithology of pebbles are primarily limestone, fine sandstone, mudstone and sandstone, etc.	The diameter of sandstone pebbles is ~5–8 cm, and pebbles are well rounded
SXC bank	27°08′53.5″	104°56′45.6″	1221	21 ± 5						The pebbles are mostly 8–15 cm in size. The lithology of pebbles are primarily limestone, fine sandstone, mudstone and sandstone, etc.	The diameter of sandstone pebbles is ~8–10 cm, and pebbles are well rounded
YTGC bank	27°06′33″	105°12′22″	1398	198 ± 5						The pebbles are mostly 5–10 cm in size. The lithology of pebbles are primarily limestone, fine sandstone, mudstone and sandstone, etc.	The diameter of sandstone pebbles is ~5–8 cm, and pebbles are well rounded

^{10}Be/^{9}Be and ^{26}Al/^{27}Al ratios were conducted in University of Glasgow. Details of experiments can be referred elsewhere (Wagner et al., 2010). The brief procedure is described as follows. Fraction with 0.125–0.25 mm size was used for quartz purification. The purified quartz (~20 g) was dissolved in a 5:1 solution of concentrated HF and HNO$_3$ and was spiked with approximately ~0.2 mg ^{9}Be. The Al and Be were extracted and separated by ion chromatography, selectively precipitated as hydroxides. The precipitates were oxidized at 800 °C. The Al$_2$O$_3$ and BeO were mixed with Ag and Nb matrix, respectively with weight ratio of Al$_2$O$_3$:Ag = 1:2 and BeO:Nb = 1:6, and then pressed into a Cu sample holder with 1 mm diameter for accelerator mass spectrometry analysis (AMS). The ^{26}Al/^{27}Al and ^{10}Be/^{9}Be ratios in the sample and procedural blanks were measured by 5MV accelerator mass spectrometer. The measured ^{26}Al/^{27}Al and ^{10}Be/^{9}Be are normalized with primary standard Z92-0222 with ^{26}Al/^{27}Al of 4.11 × 10^{-11} and NIST SRM 4325 with ^{10}Be/^{9}Be of 3.06 × 10^{-11}, respectively. In spite of the SXC sample, the measured ^{26}Al/^{27}Al and ^{10}Be/^{9}Be ratios in the other samples are in range of 10^{-13}, significantly higher than the procedural blanks with typical ratios of 10^{-15} (1 × 10^5 atoms ^{10}Be and 6 × 10^4 atoms ^{26}Al). The SXC sample has the lowest ^{26}Al/^{27}Al and ^{10}Be/^{9}Be ratios, resulting in highly correction from the procedural blanks. Stable aluminum concentrations were determined by ICP optical emission spectrometry (ICP-OES).

4.2. ^{26}Al/^{10}Be burial dating

The cosmogenic nuclides ^{26}Al and ^{10}Be were used for the cave deposit burial dating. These cosmogenic nuclides are produced in quartz near the ground surface, mostly by spallation reactions on ^{28}Si and ^{16}O. A much lesser part is produced by negative muon capture and fast muon interactions. We assume that quartz is exposed in a steadily eroded outcrop, where the pre-burial ^{26}Al/^{10}Be ratio $(N_{26}/N_{10})_0$ changes with erosion rate ε as follows:

$$\left(\frac{N_{26}}{N_{10}}\right)_0 = \frac{P_{26} \cdot (1/\tau_{10} + \rho\varepsilon/\Lambda)}{P_{10} \cdot (1/\tau_{26} + \rho\varepsilon/\Lambda)} \qquad (1)$$

where P_{26} and P_{10} are the production rate of ^{26}Al and ^{10}Be, τ_{26} and τ_{10} are the radioactive mean life of ^{26}Al and ^{10}Be ($\tau = T_{1/2}/\ln 2$; $T_{1/2}26 = 0.71$ Ma (Nishiizumi, 2004); $T_{1/2}10 = 1.39$ Ma (Chmeleff et al., 2010)), ρ is rock density (assumed 2.75 g/cm^3), ε is the rock erosion rate, Λ_n is the exponential penetration length for nucleons ($\Lambda_n \approx 160$ g/cm^2 (Masarik and Reedy, 1995)). Local cosmogenic nuclide production rates were assumed constant for the region and were calculated as $P_{10} = 10.8$ atom/(g a) and $P_{26} = 73.3$ atom/(g a) for a latitude of 27°N and an elevation of 1500 m, based on the CRONUS Earth online calculator (Version 2.2).

If the quartz is then washed deeply into the cave where it is shielded from cosmic radiation, the production of cosmogenic nuclides ceases. After burial for time t, the concentrations of ^{10}Be and ^{26}Al decay according to:

$$N_{26} = N_{26}(0)e^{-t/\tau_{26}} \qquad (2)$$

and

$$N_{10} = N_{10}(0)e^{-t/\tau_{10}}$$

because ^{26}Al decays twice as fast as ^{10}Be, the ratio N_{26}/N_{10} decreases exponentially over time according to:

$$N_{26}/N_{10} = (N_{26}/N_{10})_0 e^{-t(1/\tau_{26}-1/\tau_{10})} \qquad (3)$$

where N_{26} and N_{10} are the concentrations of ^{26}Al and ^{10}Be measured by AMS. Eqs. (1)–(3) can be solved iteratively for converging solutions of erosion rate ε and burial time t (Granger et al., 1997).

5. Results and interpretations

The cosmogenic nuclides ^{10}Be and ^{26}Al concentrations and ^{26}Al/^{10}Be ratios are shown in Table 2 and plotted in Fig. 3. The stated errors in Table 2 are 1σ calculated from AMS and ICP-OES uncertainties.

Two modern river bank cobble samples (SXC bank and YTGC bank) from the Liuchong River have burial ages of 0.26 ± 0.11 Ma and 0.35 ± 0.12 Ma respectively, implying that other samples in this area might also have experienced a complex burial history prior to their deposition in the caves. However, another modern river bank sample outside the DSC has a ^{26}Al/^{10}Be ratio of 6.68 ± 0.32, consistent with the modeled ratio of 6.76 ± 0.88 at the Earth's surface (i.e., Balco et al., 2008). This agreement suggests that the sediments experiences simple surface exposure prior to washing into the cave. Hence, no pre-burial correction has been made for cave sediments in this study.

The measured ^{26}Al/^{10}Be ratios in cave sediments yielded apparent burial ages ranging from 0.49 ± 0.13 to 2.85 ± 0.21 Ma and pre-erosion rates from 16 to 499 m/Ma (Table 2). The Dashi Cave contains the most suitable cave sediments in the study area (level A). The sediment section has the typical fluvial binary structure. The cobble burial age is 0.75 ± 0.10 Ma at the lower part of the section, whereas the overlaying sand gives 0.69 ± 0.10 Ma. Both ages overlap within the margin of uncertainty, supporting the reliability of burial age. In addition, as the rubble falling down from the ceiling covered the sediment section, it is highly considerable that the burial ages from this well-preserved section reflect the age of cave formation (Fig. 4A). Dashi Cave is controlled by the Bizhi River that is separated from the mainstem canyon by ~12 km, so the water table is still controlled by the base level of the mainstem. Field observation shows that this base level incised ~250 m since the cave was abandoned. The age of Dashi Cave most likely represents the highest level (level A) age of the Liuchong River.

Yantougou Cave (YTGC) is lower than DSC, but it still belongs to the highest level cave in this area (level A). YTGC developed ~5 km away from the main stem valley. Field observation shows that this base level incised ~90 m since the cave was abandoned. Samples were taken from gravel cemented to the conduit ceiling and wall during an episode of in-filling (Fig. 4C). As a result, the YTGC sample (0.49 ± 0.13 Ma) is interpreted as the aggradation of the Touwan River. Therefore, both DSC and YTGC samples represent an aggradation event of the Liuchong River drainage basin during 0.49–0.75 Ma.

Shenxian Cave (SXC) is in the main stem canyon wall and belongs to the fifth level (level B) of the Liuchong River. Both ^{10}Be and ^{26}Al concentrations in the sample are extremely low, resulting in a burial age of 1.46 Ma with large uncertainty (Table 2, Fig. 3). The SXC sample has significantly high pre-burial erosion rate of ~500 m/Ma (Table 2). Such a high pre-burial erosion rate indicates possibly strong erosion events around the time of sediment deposition in the cave. This is supported by the lithology of the ~5 m thickness sample profile. The sediments mainly consist of poorly sorted and subangular to subrounded cobbles (Fig. 4B). This feature can be most likely attributed in term of a great flood. This implies that the burial age of the SXC sample may not necessarily reflect a meaningful age of passage formation. The similar case has been observed in some caves in the Eastern Alps (Wagner et al., 2010). Therefore, the SXC burial age is not included in the following discussion.

Dayan Cave (DYC) is in the main stem canyon wall and belongs to the fourth level (level C) of the Liuchong River. The resulted apparent burial age is 2.85 ± 0.21 Ma and the corresponding incision rate is ~50 m/Ma. The apparent burial age is significantly older than the caves at the higher levels. The incision rate is

Table 2
Cosmogenic nuclide concentrations, ratios and sediment burial ages from caves in the Liuchong River.

Sample	Sample type	Quartz mass (g)	Be carrier (mg)	Al (ppm)	^{10}Be/^{9}Be (10^{-13})	^{26}Al/^{27}Al (10^{-13})	^{10}Be (10^3 atom/g)	^{26}Al (10^3 atom/g)	^{26}Al/^{10}Be	Burial age (Ma)	Erosion rate (m/Ma)
DSC	Sandstone pebbles	21.949	0.2157	197.6	2.913 ± 0.071	2.009 ± 0.006	188.35 ± 6.10	878.54 ± 32.22	4.66 ± 0.23	0.75 ± 0.10	22.64 ± 1.15
DSC-sand	Coarse sand	21.986	0.2177	131.9	4.216 ± 0.103	4.493 ± 0.129	276.03 ± 8.88	1317.48 ± 46.46	4.77 ± 0.23	0.69 ± 0.10	15.81 ± 0.78
YTGC	Sandstone pebbles	19.484	0.2176	190.7	1.670 ± 0.049	1.532 ± 0.068	121.33 ± 4.58	644.65 ± 32.14	5.31 ± 0.33	0.49 ± 0.13	40.21 ± 2.60
SXC	Sandstone pebbles	23.823	0.2176	242.0	0.1442 ± 0.014	0.0546 ± 0.0103	6.06 ± 1.25	20.25 ± 8.59	3.34 ± 1.58	1.46 (+1.32, −0.80)	498.91 (+245.21, −241.18)
DYC	Sandstone pebbles	20.549	0.2188	187.2	1.189 ± 0.035	0.3452 ± 0.0269	81.38 ± 3.16	137.14 ± 12.66	1.68 ± 0.17	2.85 ± 0.21	18.29 ± 1.90
DSC bank	Sandstone pebbles	23.586	0.2189	146.9	3.332 ± 0.073	4.172 ± 0.123	203.89 ± 6.20	1362.54 ± 48.93	6.68 ± 0.32	0.01 ± 0.10	30.33 ± 1.48
SXC bank	Sandstone pebbles	22.821	0.2162	155.7	1.646 ± 0.041	1.752 ± 0.058	101.32 ± 3.45	602.94 ± 23.92	5.95 ± 0.31	0.26 ± 0.11	54.13 ± 2.93
YTGC bank	Sandstone pebbles	24.446	0.2175	127.6	1.531 ± 0.045	1.781 ± 0.061	88.31 ± 3.34	502.54 ± 20.45	5.69 ± 0.32	0.35 ± 0.12	59.31 ± 3.41
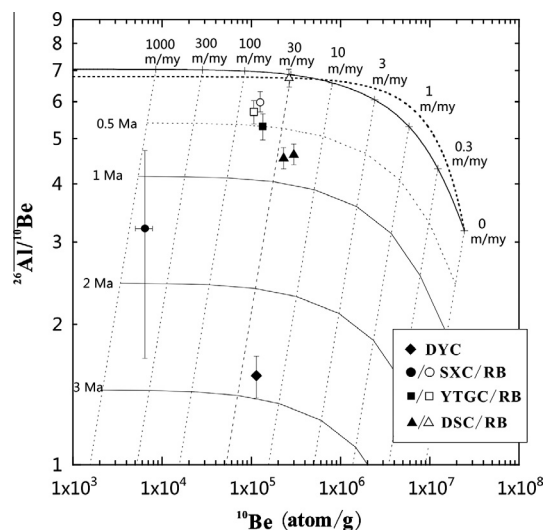
Fig. 3. Cosmogenic nuclide data from the Liuchong River buried cave sediments, shown on a logarithmic graph of ^{26}Al/^{10}Be versus ^{10}Be concentration. Labeling of sample acronyms as used in Table 1. RB: modern river bank sample outside the cave.

considerably low in comparison of other adjacent area (Clark et al., 2005; Luo et al., 2009; Wilson and Fowler, 2011; Deng, 2011). Hence, the reliability of the burial age is discussed below.

6. Discussion

6.1. Abnormal age sequence explanation

The apparent burial age of DYC at level C is significantly older than those observed in DSC and YTGC located at high level A, indicating an abnormal chronological sequence. Such an abnormal age sequence usually happens where the tectonic subsidence exists. However, the study region is considered to continuous uplift during the late Cenozoic. Excluding this possibility, we suggest that the younger ages from the higher cave level (0.75 Ma) is more reasonable based on the discussion below.

Guizhou karst topography consists of plateau and valley regions, each of which has different geomorphic evolution orientation and sequence. Plateau region is the hysteretic development area of karst topographic evolution, and the effect of river downcutting and erosion derived by the uplift has still not been reached this area entirely. The river development on the plateau region is continually to the peneplain. Conversely, the river in the valley region shows the intensive incision and headward erosion when the regional base level is lowered. And even the impact area will expand to the both sides of valley. DSC is located at the plateau region of the Liuchong River (Fig. 1B). Along the valley about 2 km west from DSC, we found a river sediment profile at about 1630 m a.s.l. (Figs. 1B and 5A). The profile is about 2 m in height, the subrounded pebbles are 5–20 cm in size. The lithology is primarily mudstone, siltstone, sandstone and limestone, which is similar with the samples from DSC and modern river. Maximal flat surface of cobbles that could indicate the head water direction are primarily face to the west, which is opposite to the modern flow direction (Fig. 5A). This observation implies that there might be a larger river that flowed across the valley from west to east in the past. Secondly, flow direction of Bizhi River is opposite to the mainstem, and it turns nearly 90° inflow to the Liuchong River (Fig. 1B). Thus, from the field investigation evidence, we argue that the Bizhi River might flow to the east together with the Liuchong River on the same altitude at first, and then the Liuchong River is
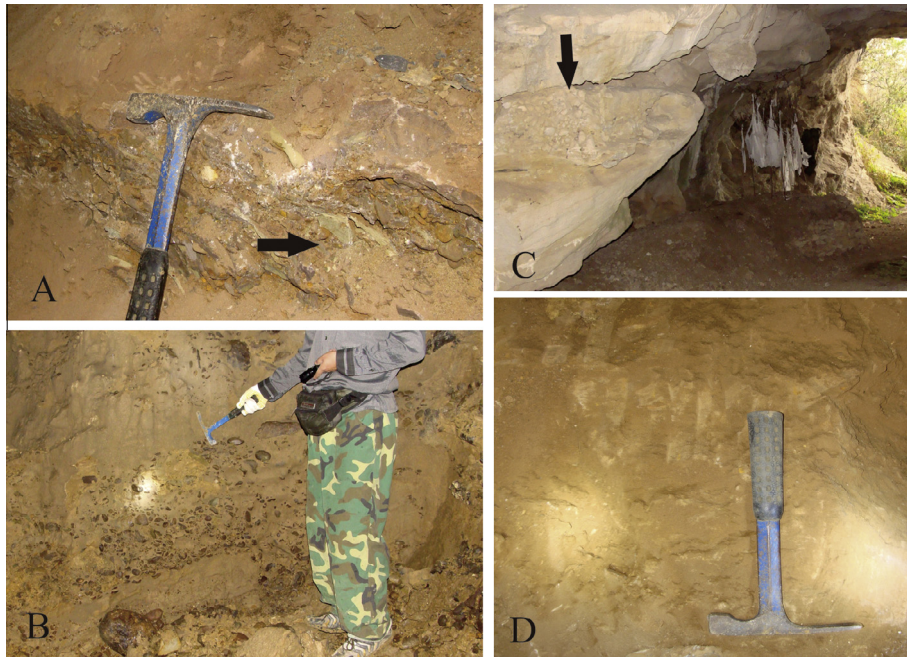
Fig. 4. Sediment samples collected from study caves. (A) Dashi Cave; (B) Shenxian Cave: different size of gravels and cobbles mixed together with good abrasion; (C) samples of Yantougou Cave are from a wall notch; (D) the size of cobbles in Dayan Cave are range from 0.5 to 3 cm and coexist with sand.

strongly downcutting when the tectonic uplift and Bizhi River is abandoned gradually. At last, a tributary of Liuchong River captures the Bizhi River, the latter changes flow direction and turns right angle debouch to the main stem. Thus, the burial ages of DSC pebble and sand may represent the last time when the conduit was an active part of the local hydrologic system. Therefore, 0.75 Ma may indicate the initial incise age of the Liuchong River and the age of this level cave and river are abandoned to keep grade with the newly lowered base level. In addition, many early Pleistocene mammalian fossil teeth have been found in the Baeryan cave located at altitude about 1630 m nearby the DSC (Zhao and Zhang, 2013). This finding supports that the age of DSC is reasonable.

The burial age of DYC is inconsistent with the field observation and landscape evolution. Firstly, there are many cobbles scattering all over the place outside the DYC, from the river bank to the altitude of Wangtian Cave. The fresh and well rounded sandstone cobbles are 2–30 cm in size and it is probably the remnant of terraces

which was eroded by the human agricultural activities (Fig. 5B). If the age of DYC is 2.85 Ma, the pebbles above the DYC elevation should older than 2.85 Ma, and the weathering degree of these cobbles would be very high according to the climate conditions (warm and wet) of Guizhou in late Cenozoic (Huang et al., 1996; Liu, 2007; Wells et al., 2008). Secondly, if the burial age of DYC truly represents the water table lowering, the incision rate of ~50 m/Ma shows a slow-paced landscape evolution in the last 2.85 Ma. It is difficult to reconcile with the landscape evolution history of Guizhou Plateau from the other evidences. Luo et al. (2009) suggests that the uplift elevation of middle part of Guizhou is nearly 1100 m in the past 5 Ma, with a uplift rate of ~220 m/Ma, according to the apatite fission track data. In comparison with this uplift rate, the low incision rate of ~50 m/Ma is considerably low. Thirdly, the regional stratum deformation (fold and fault) during the late of Early Pleistocene in China includes Yuanmou Formation in Yunnan, Nihewan Formation in Hebei, Xigeda Formation in

Fig. 5. Field impressions from related profile. (A) A river sediment profile on the left hand of road that outside the DSC, and the maximal flat surface of pebbles are shown as white dashed lines; (B) pebbles outside the DYC and the terraces are destroyed by human agricultural activities.

Sichuan, etc., which evidence that intense tectonic movement was widely developed in China at that period. This movement is nominated as Nihewan Movement in North China and Yuanmou Movement in South China, respectively. Cao et al. (1983) and Sun and Wu (1986) suggested that the movement might have happened between 1.2 and 1.5 Ma according to the magnetostratigraphy. This movement resulted in the sediment deformation of Bihenying Formation, Pingdi Formation and Xiquegou Formation in Guizhou (Lin et al., 1994). Field work shows that the strata distributed on the highest terrace of primary river valley in Guizhou, have not obviously been deformed and overlain unconformably on the Lower Pleistocene stratum. Accordingly, the formation age of the highest terrace would be younger than the Bihen Movement (1.2–1.5 Ma). Thus, these considerations make us to prefer that the DYC sample might have pre-burial history and the burial age could not represent the real information of Liuchong River. Further study of the DYC cave would clarify the alternatives.

Combining the cosmogenic nuclide ages reported here with cave level ages obtained by speleothem U-series data (Yang, 1998), we reconstruct the valley lowering history (Table 3). The cave levels of the Liuchong River are consistent with the terrace records from the adjacent areas, including Sichuan Basin, the Three Gorges area and Jianghan Basin. This implies that the evolution history of Liuchong River is generally similar as the Yangtze River since 0.75 Ma. Previous studies show the Yangtze River is developed on the base of early sectional rivers, which jointed together and reorganized drainage lines by capture and reversal (Clark et al., 2004). Then, the formation age of modern tributary drainage line should be younger than the major river. The modern Yangtz River is considered to have found after the cut through of Three Gorges. The cut through age of Three Gorges are approximately 0.7–1.2 Ma based on ESR ages of sediment in Yichang and paleomagnetism dates from drilling deposit in Jianghan Plain and Changjiang Delta (Yang et al., 2006; Zhang et al., 2008; Wang et al., 2009; Xiang et al., 2005, 2006, 2007, 2011). These data suggest that the initial age of modern Wujiang River would be younger than 0.7–1.2 Ma. Furthermore, geological evidence has confirmed that the age of fluvial terraces should be after the end of early Pleistocene (Lin et al., 1994). Considering that Liuchong River is the northern origin of Wujiang River, we suggest that the initial formation age of modern Wujiang River is most likely 0.75 Ma ago.

6.2. Comparison with other river incision rates

The mean incision rate of the Liuchong River documented by cosmogenic nuclides is ~0.48 m/ka during the last 0.75 Ma. This value is significantly higher than those observed in other adjacent localities. For example, it is apparently higher than the mean incision rates of the Dadu River, Xianshui River and Zagunao River (~0.37–0.39 m/ka) at the eastern margin of Tibetan Plateau during the Pleistocene, obtained by terrace ESR datas (Liu, 2006). Furthermore, Ouimet et al. (2010) used U–Th/He analyses at the eastern margin of Tibetan Plateau shows that the Dadu River, Yalong River and Yangtz River are incising at about 0.33 m/ka, 0.34 m/ka and

0.38 m/ka over 10 Ma, respectively. Our data are also 2–3 times higher than the incision rate of rivers at the northeastern Tibetan Plateau. Pan et al. (2003) reported a bedrock incision rate of ~0.14 m/ka over the past 0.87 Ma based on TL dates of paleosols from the terraces of Shagou River in the Qilian Mountains. Using paleomagnetism, OSL and ¹⁴C methods, Pan et al. (2007) suggests that the incision rate of Wei River, which has flowed over the northern part of Qinling Mountain, is ~0.2 m/ka during the last 0.87 Ma.

The ages of speleothems estimated by the U-series might be younger than the burial ages of gravels (Stock et al., 2005a). Therefore, the incision rates inferred from the speleothem U-series ages might lead to overestimates of the river incision rates. A more detailed analysis of the data suggests that the incision rate of the Liuchong River was initially high (~0.55 m/ka) and recently low (~0.21 m/ka). This pattern is unconsistent with the fact that there is a tendency of intensive recent uplift. The mean river downcutting rate of the Three Gorges area of the Yangtze River was ~0.25 m/ka in the past 0.4 Ma (Yang et al., 2002), and increased to ~0.81 m/ka since 0.13 Ma ago (Zhou et al., 2006). The incision rate from the U series age in Bubing Basin of western Guangxi is approximately 0.14 m/ka in the past 0.29 Ma (Wang et al., 2007), which is lower than Liuchong River during the last 0.18 Ma. Moreover, the incision rate of Liuchong River since 48 ka (~0.21 m/ka) is much lower than those of the Minjiang River, Jinshajiang River and Yellow River in the same period (~0.77–2.65 m/ka) (Yang et al., 1996; Li et al., 2005, 2006; Ge et al., 2006).

The multilevel caves and alluvial terraces are the result of tectonic uplift and base level lowering. When the river incision equals rock uplift, the incision rate calculated from terrace or cave could represent the rock uplift rate. Thus, fluvial incision and terrace are possibly the part result of tectonic uplift, and uplift rate calculated from elevated terraces or caves merely yield the maximum value (Kiden and Tornqvist, 1998). However, it is worth to mention the possible mechanisms for this intensive river incision rate. It seems unreasonable that the river incision rate from northwestern Guizhou is higher than the rivers on the west margin of Sichuan, which is clearly affected by uplift of the Tibetan Plateau. Although we do not have a convincing explanation for this interesting discrepancy at present, we consider two possibilities as follows. One is the both effect of cut-through of the Three Gorges (~0.75 Ma (Xiang et al., 2007)) that may lowering the regional base level, and the uplift of Tibetan Plateau which may increase the rock elevation (GGMB, 1987; Zhou and Chen, 1993; Lin et al., 1994; Li, 2001; Xiang, 2004). The cut-through of Three Gorges is an important event for the whole Yangtze River drainage basin, not only reorganize the river system, but also strengthen lowering the regional base level and make intensive head erosion of the Wujiang River. Another possibility is the difference of bedrock lithology. The bedrock types of eastern Tibetan Plateau and western Guizhou are mainly clastic and silicate rocks, and carbonate rocks, respectively. In general, silicate rocks have higher resistance to incision than carbonate rocks. However, the floodplain lowering rate of Guilin karst area is lower than 23 m/Ma during the last 0.9 Ma (Williams,

Table 3
Chronology derived from the Liuchong River and the comparison with the adjacent areas (ages are listed from old to young).

Liuchong River						Other localities (Sichuan Basin, Three Gorges and Jianghan Basin)		
Level	Terrace	Height above local river (m)	Age (Ma)	Dating method	Data source	Terrace	Age (Ma) (Li, 2001)	Age (Ma) (Xiang, 2004)
A	T4	340–360	0.75–0.49	TCN	By authors	T5	0.73	0.7–0.73
B		220–250	–					
C	T3	120–140	>0.35	U-series	Yang (1998)	T4	0.49	0.3–0.5
D		58–71	0.16–0.18	U-series	Yang (1998)	T3	0.15	0.09–0.11
E	T2	25–30	–	U-series	Yang (1998)	T2	0.0586	0.03–0.05
F	T1	5–10	0.048	U-series	Yang (1998)	T1	0.031	0.01

1987). This result is significantly lower than our data, probably due to the different karst landscape evolution patterns. It should be pointed out that Guilin is a peak forest plain with average elevation is ~150 m, whose landscape evolution is going to be a penelain. However, generally speaking, landscape evolution in Guizhou is vertical developing that is suitable for the constant lowering of base level during the late Cenozoic.

7. Conclusions

The cosmogenic nuclide burial dating from the multilevel cave sediments of the Liuchong River was made. The northern origin of Wujiang River shows that the river incised the bedrock some 350–400 m in the last 0.75 Ma, recorded a complex incision history resulting in a mean incision rate of ~480 m/Ma. This river incision rate is higher than many rivers around the eastern and northeastern margin of Tibetan Plateau at the same period, which might be explained by factors such as difference of bedrock lithology, the uplift of the Tibetan Plateau and the base level lowering caused by the cut-through of Three Gorges. Together with the published U-series ages of speleothems, a river incision history was established for the Liuchong River. The development of Liuchong River is generally similar as the Yangtze River, which indicates that the embryonic form of modern Wujiang River was possibly presented at 0.75 Ma ago.

Acknowledgements

References

Anthony, D.M., Granger, D.E., 2004. A Late Tertiary origin for multilevel caves along the western escarpment of the Cumberland Plateau, Tennessee and Kentucky, established by cosmogenic ^{26}Al and ^{10}Be. Journal of Cave and Karst Studies 66, 46–55.

Anthony, D.M., Granger, D.E., 2007. A new chronology for the age of Appalachian erosional surfaces determined by cosmogenic nuclides in cave sediments. Earth Surface Processes and Landforms 32, 874–887.

Balco, G., Rovey, C.W., 2008. An isochron method for cosmogenic nuclide dating of buried soils and sediments. American Journal of Science 308, 1083–1114.

Balco, G., Stone, J.O.H., Jennings, C., 2005. Dating Plio-Pleistocene glacial sediments using the cosmic-ray-produced radionuclides ^{10}Be and ^{26}Al. American Journal of Science 305, 1–41.

Balco, G., Stone, J.O., Lifton, N.A., Dunai, T.J., 2008. A complete and easily accessible means of calculating surface exposure ages or erosion rates from ^{10}Be and ^{26}Al measurements. Quaternary Geochronology 3, 174–195.

Cao, Z.Y., Yu, Q.H., Liu, L.S., He, P.Y., 1983. Problems concerning the Lower Limit of Quaternary in China. Acta Geological Sinica 1, 96–103 (in Chinese).

Chmeleff, J., Blanckenburg, F., Kossert, K., Jakob, D., 2010. Determination of the ^{10}Be half-life by multicollector ICP-MS and liquid scintillation counting. Nuclear Instruments and Methods in Physics Research Section B 268, 192–199.

Clark, M.K., Schoenbohm, L.M., Royden, L.H., Whipple, K.X., Burchfiel, B.C., Zhang, X., Tang, W., Wang, E., Chen, L., 2004. Surface uplift, tectonics, and erosion of eastern Tibet from large-scale drainage patterns. Tectonics 23, 1–20.

Clark, M.K., House, M.A., Royden, L.H., Whipple, K.X., Burchfiel, B.C., Zhang, X., Tang, W., 2005. Late Cenozoic uplift of southeastern Tibet. Geology 33, 525–528.

Deng, X.D., 2011. Late Cenozoic Supergene Enrichment of Manganese Oxide Deposits throughout the Yunnan-Guizhou Plateau and Adjacent Area: Implications for the Plateau Uplift and Paleoclimatic Conditions. PhD Thesis, China University of Geosciences, Beijing, China (in Chinese).

Enlanger, E.D., Granger, D.E., Gibbon, R.J., 2012. Rock uplift rates in South Africa from isochron burial dating of fluvial and marine terraces. Geology 40, 1019–1022.

Ge, Z.S., Liu, Q.Y., Xu, Q.M., Li, H.Z., Xue, G.F., Mei, Y.T., Xu, Y.H., 2006. The geomorphic evolution and characteristics of the river bed in the lower reaches of Jinshajiang River. Quaternary Sciences 26, 421–428 (in Chinese).

Guizhou Geology Mineral Bureau, 1987. Regional Geology of Guizhou. Geology Press, Beijing, pp. 599–607.

Granger, D.E., Kirchner, J.W., Finkel, R.C., 1997. Quaternary downcutting rate of the New River, Virginia, measured from differential decay of cosmogenic ^{26}Al and ^{10}Be in cave-deposited alluvium. Geology 25, 107–110.

Granger, D.E., Fabel, D., Palmer, A.N., 2001. Pliocene–Pleistocene incision of the Green River, Kentucky, determined from radioactive decay of cosmogenic ^{26}Al and ^{10}Be in Mammoth Cave sediments. Geological Society of America Bulletin 113, 825–836.

Haeuselmann, P., Granger, D.E., Jeannin, P.Y., Lauritzen, S.E., 2007. Abrupt glacial valley incision at 0.8 Ma dated from cave deposits in Switzerland. Geology 35, 143–146.

Hu, X.F., Kirby, E., Pan, B.T., Granger, D.E., Su, H., 2011. Cosmogenic burial ages reveal sediment reservoir dynamics along the Yellow River, China. Geology 39, 839–842.

Huang, Z.G., Zhang, W.Q., Chen, J.H., Liu, R.H., He, Z.Y., 1996. Red Weathering Crust of South China. Ocean Press, Beijing, pp. 166–167 (in Chinese).

Kiden, P., Tornqvist, T.E., 1998. Can river terrace flights be used to quantify Quaternary tectonic uplift rates? Journal of Quaternary Science 13, 573–575.

Kong, P., Granger, D.E., Wu, F.Y., Caffee, M.W., Wang, Y.J., Zhao, X.T., Zheng, Y., 2009. Cosmogenic nuclide burial ages and provenance of the Xigeda paleo-lake: implications for evolution of the Middle Yangtze River. Earth and Planetary Science Letters 278, 131–141.

Li, X.Z., 2001. Evolution of karst geomorphology of upper Cenozoic and its influential factors in Guizhou Plateau. Guizhou Geology 18, 29–36 (in Chinese).

Li, Y., Cao, S.Y., Zhou, R.J., Densmore, A.L., Ellis, M.A., 2005. Late Cenozoic Min Jiang incision rate and its constraint on the uplift of the eastern margin of the Tibetan Plateau. Acta Geologica Sinica 79, 28–37 (in Chinese).

Li, Y., Densmore, A.L., Zhou, R.J., Ellis, M.A., Zhang, Y., Li, B., 2006. Profiles of digital elevation models (DEM) crossing the eastern margin of the Tibetan Plateau and their constraints on dissection depths and incision rates of Late Cenozoic rivers. Quaternary Sciences 26, 236–243 (in Chinese).

Li, M.Q., Wang, Z.Y., Qian, R., Xu, J., Huang, X.G., Lai, K.D., 2007. Evolution of karst desertification in response to Neotectonism in Western Guizhou. Journal of Guizhou University (Natural Sciences) 24, 322–326 (in Chinese).

Lin, S.J., Zhou, Q.Y., Chen, P.Y., 1994. The Upper Cainozoic of Guizhou. Guizhou Science and Technology Press, Guiyang, pp. 66–126 (in Chinese).

Liu, Y., 2006. Study of the Step-like Landforms in Western Sichuan Plateau, China. MS Thesis, Nanjing Normal University, pp. 29–45 (in Chinese).

Liu, C.Q., 2007. Biogeochemistry Process and Surface Material Cycle – Karst drainage Basin Erosion and Biogenic Factors Cycle of Southwestern China. Science Press, Beijing, pp. 151–152 (in Chinese).

Luo, K.P., Liu, G.X., Wang, J.Y., 2009. Fission track analysis of Meso-Cenozoic Uplift and denudation in Jinsha Area, the Qianzhong Uplift. Marine Origin Petroleum Geology 14, 61–64 (in Chinese).

Masarik, J., Reedy, R.C., 1995. Terrestrial cosmogenic nuclide production systematic calculated from numerical simulations. Earth and Planetary Science Letters 136, 381–395.

Matmon, A., Schwartz, D., Finkel, R., Clemmens, S., Hanks, T., 2005. Dating offset fans along the Mojave section of the San Andreas fault using cosmogenic ^{26}Al and ^{10}Be. Geological Society of America Bulletin 117, 795–807.

Matmon, A., Stock, G.M., Granger, D.E., Howard, K.A., 2012. Dating of Pliocene Colorado River sediments: implications for cosmogenic burial dating and the evolution of the lower Colorado River. Geological Society of America Bulletin 124, 626–640.

Nishiizumi, K., 2004. Preparation of ^{26}Al AMS standards. Nuclear Instruments and Methods in Physics Research Section B 223, 388–392.

Ouimet, W., Whipple, K., Royden, L., Reiners, P., Hodges, K., Pringle, M., 2010. Regional incision of the eastern margin of the Tibetan Plateau. Lithosphere 2, 50–63.

Pan, B.T., Burbank, D., Wang, Y.X., Wu, G.J., Li, J.J., Guan, Q.Y., 2003. A 900 k.y. record of strath terrace formation during glacial–interglacial transitions in northwest China. Geology 31, 957–960.

Pan, B.T., Liu, X.F., Gao, H.S., Wang, Y., Li, J.J., 2007. Forming age and cause of fluvial terraces at Longxi reach of Wei River. Advances in Earth Science 17, 1063–1068 (in Chinese).

Partriage, T.C., Granger, D.E., Caffee, M.W., Clarke, R.J., 2003. Lower Pliocene hominid remains from Sterkfontein. Science 300, 607–612.

Stock, G.M., Granger, D.E., Sasowsky, I.D., Anderson, R.S., Finkel, R.C., 2005a. Comparison of U–Th, paleomagnetism, and cosmogenic burial methods for dating caves: implications for landscape evolution studies. Earth and Planetary Science Letters 236, 388–403.

Stock, G.M., Anderson, R.S., Finkel, R.C., 2005b. Rates of erosion and topographic evolution of the Sierra Nevada, California, inferred from cosmogenic ^{26}Al and ^{10}Be concentrations. Earth Surface Processes and Landforms 30, 985–1006.

Sun, D.Q., Wu, X.H., 1986. A preliminary study of Quaternary Tectono-climatic cycles in China. Quaternary Science 7, 1–9 (in Chinese).

Wagner, T., Fabel, D., Fiebig, M., Häuselmann, P., Sahy, D., Xu, S., Stüwe, K., 2010. Young uplift in the non-glaciated parts of the Eastern Alps. Earth and Planetary Science Letters 295, 159–169.

Wang, W., Potts, R., Yuan, B.Y., Huang, W.W., Cheng, H., Edwards, R.L., Ditchfield, P., 2007. Sequence of mammalian fossils, including hominoid teeth, from the Bubing Basin caves, South China. Journal of Human Evolution 52, 370–390.

Wang, Q.L., Hu, S.H., Li, C.A., 2009. Heavy mineral characteristics of gravel layers in the Zhoulao Town borehole. Geology in China 36, 878–884 (in Chinese).

Wells, T., Hancock, G., Fryer, J., 2008. Weathering rates of sandstone in a semi-arid environment (Hunter Valley, Australia). Environmental Geology 54, 1047–1057.

Williams, P.W., 1987. Geomorphic inheritance and the development of tower karst. Earth Surface Processes and Landforms 12, 453–465.

Wilson, C.J.L., Fowler, A.P., 2011. Denudational response to surface uplift in east Tibet: evidence from apatite fission-track thermochronology. Geological Society of America Bulletin 123, 1966–1987.

Wolkowinsky, A.J., Granger, D.E., 2004. Early Pleistocene incision of the San Juan River, Utah, dated with ^{26}Al and ^{10}Be. Geology 32, 749–752.

Xiang, F., 2004. Forming of the Three Gorges of the Yangtze River and Sedimentary response in the West Edge of Jianghan Basin and Adjacent Area. PhD Thesis, Chengdu University of Technology, Chengdu, pp. 90–97 (in Chinese).

Xiang, F., Zhu, L.D., Wang, C.S., Li, Y.Z., Yang, W.G., 2005. Terrace age correlation and its significance in research of Yangtze Three Gorges, China. Journal of Chengdu University of Technology (Science and Technology Edition) 32, 162–166 (in Chinese).

Xiang, F., Wang, C.S., Li, G.Z., Zhu, L.D., Li, Y.Z., Jiang, P., 2006. Character of heavy minerals in Quaternary sediments in Yichang area and its relationship with cut-through of the Yangtze Three Gorges, China. Journal of Chengdu University of Technology (Science and Technology Edition) 33, 117–121 (in Chinese).

Xiang, F., Zhu, L.D., Wang, C.S., Zhao, X.X., Chen, H.D., Yang, W.G., 2007. Quaternary sediment in the Yichang area: implications for the formation of the Three Gorges of the Yangtze River. Geomorphology 85, 249–258.

Xiang, F., Yang, D., Tian, X., Li, Z.H., Luo, X., 2011. LA-ICP-MS U–Pb geochronology of zircons in the Quaternary sediments from the Yichang area of Hubei province and its provenance significance. Journal of Mineral Petrology 31, 106–114 (in Chinese).

Yang, H.R., 1944. Landform development of middle part of Guizhou. Acta Geographica Sinica 11 (in Chinese).

Yang, M.D., 1998. Development of cavities in karstic valley in respondent to hydrodynamics 15, 17–25 (in Chinese).

Yang, D.Y., Wu, S.G., Wang, Y.F., 1996. On river terraces of the upper reaches of the Huanghe River and change of the river system. Scientia Geographica Sinica 16, 137–143 (in Chinese).

Yang, D.Y., Li, X.S., Feng, L.M., Jiang, H.T., 2002. Pilot study on the collapses and landslides of the Three Gorge Reservoir of the Changjiang River. Journal of Geomechanics 8, 173–178 (in Chinese).

Yang, S.Y., Li, C.X., Yokoyama, K., 2006. Elemental compositions and monazite age patterns of core sediments in the Changjiang Delta: implications for sediment provenance and development history of the Changjiang River. Earth and Planetary Science Letters 245, 762–776.

Zhang, S.Y., Zhao, S.S., 1985. Radioactive Dating of Shenxian Cave Sediments from Dushan, Guizhou. Karst Landform and Cave. Science Press, Beijing, pp. 113–116 (in Chinese).

Zhang, Y.F., Li, C.A., Wang, Q.L., Chen, L., Ma, Y.F., Kang, C.G., 2008. Magnetism parameters characteristics of drilling deposits in Jianghan Plain and indication for forming of the Yangtze River Three Gorges. Chinese Science Bulletin 53, 584–590.

Zhao, L.X., Zhang, L.Z., 2013. New fossil evidence and diet analysis of *Gigantopithecus blacki* and its distribution and extinction in South China. Quaternary International 286, 69–74.

Zhou, Q.Y., Chen, P.Y., 1993. Lithofacies change and palaeogeographical evolution during late Cenozoic in Guizhou and its Vicinity. Guizhou Geology 10, 201–207 (in Chinese).

Zhou, B., Yang, D.Y., Han, Z.Y., Li, X.S., Wang, P., Ge, Z.S., 2006. Incision rate of the Three Gorges section of the Changjiang River. Quaternary Science 26, 406–412 (in Chinese).